



# Role of Contrast-Enhanced Ultrasound as a Second-Line Diagnostic Modality in Noninvasive Diagnostic Algorithms for Hepatocellular Carcinoma

Hyo-Jin Kang, MD<sup>1, 2</sup>, Jeong Min Lee, MD, PhD<sup>1, 2, 3</sup>,  
Jeong Hee Yoon, MD, PhD<sup>1, 2</sup>, Joon Koo Han, MD, PhD<sup>1, 2, 3</sup>

<sup>1</sup>Department of Radiology, Seoul National University Hospital, Seoul, Korea; <sup>2</sup>Department of Radiology, Seoul National University College of Medicine, Seoul, Korea; <sup>3</sup>Institute of Radiation Medicine, Seoul National University Medical Research Center, Seoul, Korea

**Objective:** To investigate the diagnostic performance of contrast-enhanced ultrasound (CEUS) and its role as a second-line imaging modality after gadoxetate-enhanced MRI (Gd-EOB-MRI) in the diagnosis of hepatocellular carcinoma (HCC) among at risk observations.

**Materials and Methods:** We prospectively enrolled participants at risk of HCC with treatment-naïve solid hepatic observations ( $\geq 1$  cm) of Liver Imaging Reporting and Data System (LR)-3/4/5/M during surveillance and performed Gd-EOB-MRI. A total of one hundred and three participants with 103 hepatic observations (mean size,  $28.2 \pm 24.5$  mm; HCCs [ $n = 79$ ], non-HCC malignancies [ $n = 15$ ], benign [ $n = 9$ ]; diagnosed by pathology [ $n = 57$ ], or noninvasive method [ $n = 46$ ]) were included in this study. The participants underwent CEUS with sulfur hexafluoride. Arterial phase hyperenhancement (APHE) and washout on Gd-EOB-MRI and CEUS were evaluated. The distinctive washout in CEUS was defined as mild washout 60 seconds after contrast injection. The diagnostic ability of Gd-EOB-MRI and of CEUS as a second-line modality for HCC were determined according to the European Association for the Study of the Liver (EASL) and the Korean Liver Cancer Association and National Cancer Center (KLCA-NCC) guidelines. The diagnostic abilities of both imaging modalities were compared using the McNemar's test.

**Results:** The sensitivity of CEUS (60.8%) was lower than that of Gd-EOB-MRI (72.2%,  $p = 0.06$  by EASL; 86.1%,  $p < 0.01$  by KLCA-NCC); however, the specificity was 100%. By performing CEUS on the inconclusive observations in Gd-EOB-MRI, HCCs without APHE ( $n = 10$ ) or washout ( $n = 12$ ) on Gd-EOB-MRI further presented APHE (80.0%, 8/10) or distinctive washout (66.7%, 8/12) on CEUS, and more HCCs were diagnosed than with Gd-EOB-MRI alone (sensitivity: 72.2% vs. 83.5% by EASL,  $p < 0.01$ ; 86.1% vs. 91.1% by KCLA-NCC,  $p = 0.04$ ). There were no false-positive cases for HCC on CEUS.

**Conclusion:** The addition of CEUS to Gd-EOB-MRI as a second-line diagnostic modality increases the frequency of HCC diagnosis without changing the specificities.

**Keywords:** Hepatocellular carcinoma; Liver; Magnetic resonance imaging; Contrast enhanced ultrasound

## INTRODUCTION

Hepatocellular carcinoma (HCC) can be diagnosed noninvasively, and treatment may be initiated based on

imaging alone because of its high pretest probability and the high positive-predictive value of the HCC imaging criteria in cirrhotic participants (1). Imaging is important in HCC screening, surveillance, diagnosis, staging, and

**Received:** June 3, 2020 **Revised:** August 3, 2020 **Accepted:** September 5, 2020

This study was supported by a research grant (no. 0620183430) from Bracco Imaging (Milan, Italy). We thank to Hyun Hee Lee (Seoul National University Hospital, Korea) for her assistant.

**Corresponding author:** Jeong Min Lee, MD, PhD, Department of Radiology, Seoul National University College of Medicine, 101 Daehak-ro, Jongno-gu, Seoul 03080, Korea.

• E-mail: [jmsh@snu.ac.kr](mailto:jmsh@snu.ac.kr)

This is an Open Access article distributed under the terms of the Creative Commons Attribution Non-Commercial License (<https://creativecommons.org/licenses/by-nc/4.0>) which permits unrestricted non-commercial use, distribution, and reproduction in any medium, provided the original work is properly cited.

management (2-4). Clinical practice guidelines, including those of the Association for the Study of Liver Disease (AASLD) (1), European Association for the Study of the Liver (EASL) (5), and the Korean Liver Cancer Association and National Cancer Center (KLCA-NCC) (6), recommend contrast-enhanced CT and MRI for HCC diagnosis (7). However, these guidelines differ regarding the use of contrast-enhanced ultrasound (CEUS) for HCC. The AASLD does not include CEUS, whereas the EASL and KLCA-NCC guidelines recommend CEUS as a second-line diagnostic modality. CEUS with sulfur hexafluoride has shown to improve noninvasive HCC diagnosis when initial modalities, such as CECT or MRI with extracellular contrast agents or hepatobiliary agent, do not show hallmark HCC features (7, 8).

By real-time imaging, CEUS sensitively depicts arterial hypervascularity, reducing the clinical need for invasive biopsies that are otherwise required for indeterminate nodules (9-11). Furthermore, CEUS allows the differentiation of vascular pseudolesions from atypically enhancing HCC, as the former are absent on CEUS (7, 12-16). Earlier studies have reported that approximately 50% of mass-forming cholangiocarcinomas (CCs) in cirrhosis showed arterial-phase hyperenhancement (APHE) followed by washout on CEUS, leading to misdiagnosis of HCC (17, 18). However, subsequent studies (8, 19-21) have demonstrated that many HCCs showed APHE followed by late ( $\geq 60$  seconds) and mild washout (22, 23), while many CCs showed APHE followed by early ( $< 60$  seconds) or marked washout (19, 20) on CEUS. These diagnostic criteria are highly specific for the diagnosis of HCC, and Terzi et al. (24) reported a 98.5% positive predictive value for the diagnosis of HCC among 1006 at risk nodules (5, 7, 24). Furthermore, CEUS showed high specificity, with only a slight drop in sensitivity for 10–20 mm nodules, after initial inconclusive results on CECT or dynamic MRI (7). However, to date, no study has explored the diagnostic value of CEUS after inconclusive gadoxetate-enhanced MRI (Gd-EOB-MRI). We hypothesized that CEUS would have a different diagnostic ability from Gd-EOB-MRI, and this difference would help diagnose HCC on an inconclusive observation on Gd-EOB-MRI. To investigate this hypothesis, we compared the diagnostic performance of Gd-EOB-MRI alone and Gd-EOB-MRI followed by CEUS. Therefore, this study aimed to evaluate the diagnostic ability of CEUS with sulfur hexafluoride to diagnose HCC after an inconclusive observation in Gd-EOB-MRI and to establish the role of CEUS as a second-line (post-Gd-EOB-

MRI) modality for the diagnosis of HCC.

## MATERIALS AND METHODS

This prospective study was approved by the Institutional Review Board of our institute, and all participants provided written informed consent (IRB No. 1807-166-962).

### Participants

From November 2018 to August 2019, participants who met the following criteria were included in the study: age  $\geq 18$  years; at risk of HCC by the Liver Imaging Reporting and Data System (LI-RADS) v2018 (25) (liver cirrhosis or chronic hepatitis B viral infection), and at least one treatment-naïve solid hepatic observation ( $\geq 1$  cm) of LR-3/4/5/M by CT/MRI LI-RADS v2018 in CT or MRI. Exclusion criteria were refusal to consent, congestive hepatopathies, obvious tumor in vein severe cardiovascular dysfunction, no Gd-EOB-MRI within four weeks pre-CEUS, and suboptimal Gd-EOB-MRI quality (Fig. 1, Table 1). Liver cirrhosis was proven by histopathologic results or stiffness values of transient elastography (26, 27). When Gd-EOB-MRI presented multiple eligible observations, one representative per participant was analyzed (28) following predetermined criteria: 1) an observation possessing a higher probability of hepatic malignancy according to CT/MRI LI-RADS v2018., 2) closer to the skin, 3) better visibility on B-mode ultrasound (US), and 4) manageable tumor size ( $< 12$  cm, considering scan coverage of a convex US probe).

One hundred and seven participants were enrolled in the study. Among them, four participants were excluded for insufficient diagnosis, referring to an inconclusive histopathologic diagnosis ( $n = 2$ ), or did not meet the noninvasive diagnostic criteria of HCC ( $n = 2$ ). Accordingly, 103 observations in 103 participants (81 men; mean age,  $63.1 \pm 10$  years; range, 21–86 years) were finally included in our study (Fig. 1).

### Gd-EOB-MRI Acquisition

MRI was performed using 3T (99.0%,  $n = 101$ ) or 1.5T (1.0%,  $n = 2$ ) scanners (see details in Supplementary Materials). A standard dose (0.1 mL/kg) of gadoxetate disodium (Primovist, Bayer AG) was administered at 1 mL/s, followed by a 20-mL saline flush. For dynamic sequences, arterial phase was obtained 7–8 seconds after contrast media arrived at the descending thoracic aorta, using real-time MR fluoroscopic monitoring. Thereafter, 3 dimensional

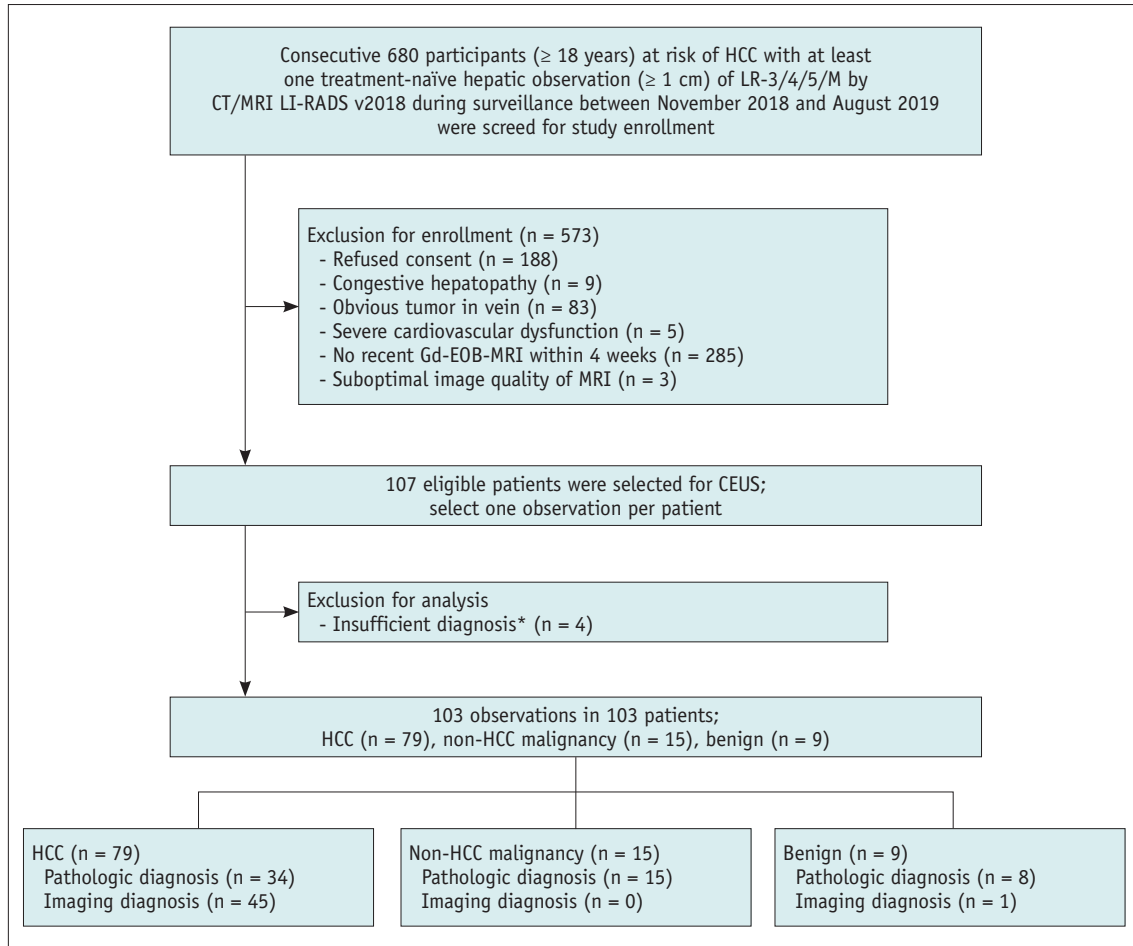


**Fig. 1. Flow diagram of the participants included in the study.** \*Inconclusive histopathologic diagnosis (n = 2), or lack of long term follow up (≥ 2 years) to assure benignity (n = 2). CEUS = contrast-enhanced ultrasound, Gd-EOB-MRI = gadoxetate-enhanced MRI, HCC = hepatocellular carcinoma, LI-RADS = Liver Imaging Reporting and Data System, LR = LI-RADS

fat-suppressed T1-weighted gradient-echo portal venous (PVP), transitional, and hepatobiliary phase (HBP) were obtained at 55–65-seconds, 3-minutes, and 20-minutes after contrast media injection.

### CEUS Examination

CEUS was performed by one of two fellowship-trained radiologists with 24- and 8-years' experience in abdominal US and 11 and 4 years' experience in CEUS, respectively, using a contrast-specific US platform with a convex probe (Supplementary Materials). Operators could adjust US parameters to optimally depict observations. All B-mode and CEUS images were displayed side-by-side on a USG monitor. Details of the US parameters are shown in Supplementary Table 1. For small (< 1.5 cm) or indistinguishable lesions, real-time US images were fused with CT/MRI for accurate examination (n = 46, 45.5%). Sulfur hexafluoride (SonoVue, Bracco) was prepared according to the manufacturer's

recommendations. Sulfur hexafluoride (2.4 mL) was manually injected via an antecubital venous line and flushed with 10 mL normal saline. The timer was started at the beginning of the saline flush (22). Continuous CEUS images of the target were recorded for the first 60 seconds post-contrast injection followed by intermittent scans every 15 seconds for 5 minutes after contrast media administration.

### Image Analysis

Two board-certified radiologists with 13- and 8-years' experience in liver MRI and 9 and 4-years' experience in CEUS, respectively, independently reviewed MR and saved CEUS images. They were blinded to the pathology results and clinical or laboratory information; however, they knew that the study population was at risk for HCC and were given the size and location of each target observation. Reviewers assessed the presence of major imaging features of HCC (APHE, washout, and capsule appearance) as well

**Table 1. Clinicopathologic Characteristics of 103 Participants with 103 Observations**

Participants	n = 103
Mean age	63.1 (21–86)
Sex	
Male:female	81:22
Cause of liver diseases	
Hepatitis B virus	67 (65)
Hepatitis C virus	6 (5.8)
Alcohol	11 (10.7)
Others	19 (18.3)
Known cirrhosis	45 (43.7)
Child-Pugh classification	
A	95 (92.2)
B	8 (7.8)
AFP level (ng/mL)*	8.2 (1.1–7466)
PIVKA (mAU/mL)*	35 (11–43913)
Observations	n = 103
Size (mm)	28.2 (11–114)
10–19	58 (56.3)
≥ 20	45 (43.7)
CT/MRI LI-RADS category	
LR-3	5 (4.9)
LR-4	21 (20.4)
LR-5	60 (58.3)
LR-M	17 (16.5)
Final diagnosis	
HCC	79 (76.7)
Non-HCC malignancy	
cHCC-CC	2 (1.9)
IHCC	11 (10.6)
Angiosarcoma	1 (1)
Metastasis	1 (1)
Benign	
Dysplastic nodule	3 (2.9)
Adenoma	2 (1.9)
Regenerative nodule	1 (1)
Hemangioma	1 (1)
Focal nodular hyperplasia	1 (1)
Organizing hematoma	1 (1)
Reference standard for diagnosis	
Pathological diagnosis	57 (55.3)
Noninvasive	45 (43.7)
Typical image features with more than 1-year stability <sup>†</sup>	1 (1)

\*Median value, <sup>†</sup>Only for diagnosing hemangioma that presented peripheral globular enhancement pattern on CT and MRI with stability (> 1-year). AFP = alpha-fetoprotein, cHCC-CC = combined hepatocellular-cholangiocarcinoma, HCC = hepatocellular carcinoma, IHCC = intrahepatic cholangiocarcinoma, LI-RADS = Liver Imaging Reporting and Data System, LR = LI-RADS, PIVKA = protein induced by vitamin K absence or antagonist

as other malignancy features (targetoid appearance on dynamic phase including rim APHE) on Gd-EOB-MRI. The definition of major imaging features of the EASL and KLCA-NCC guidelines and their diagnostic criteria are listed in Table 2.

To avoid recall bias, for CEUS 2-weeks post-MRI review, the reviewers also recorded the major imaging features, which included APHE with its pattern (rim vs. non-rim and non-peripheral globular), and timing (early or late) and degree (mild or marked) of washout. The definitions of APHE and washout are presented in Table 2. The distinctive washout of HCC on CEUS refers to the mild washout 60 seconds after contrast injection. The CEUS criteria for noninvasive diagnosis of HCC were hepatic observation (≥ 1 cm) with non-rim APHE and mild washout after 60 seconds, following the EASL and KLCA-NCC guidelines (5, 6, 22).

### Reference Standard

Diagnosis was based on pathology or characteristic imaging features. One of the two experienced pathologists (with more than 17 and 19-years' experience in hepatic pathology) made pathological diagnoses. For the radiologic diagnosis of HCC, we used CECT findings based on the CT/MRI LI-RADS v2018 (25). Hemangioma (n = 1) was diagnosed by characteristic imaging features on CECT, which referred to a peripheral globular, centripetal enhancement pattern that remained stable in size during follow-up.

### Statistical Analysis

The diagnostic performance of Gd-EOB-MRI and CEUS for HCC, following the EASL and KLCA-NCC guidelines, were compared accordingly. Thereafter, to simulate the role of CEUS as a second-line diagnostic modality, all observations were applied to the diagnostic algorithms of EASL and KLCA-NCC: 1) evaluation by Gd-EOB-MRI as a first-line diagnostic modality and 2) evaluation by CEUS for inconclusive observation on Gd-EOB-MRI.

The presence of APHE or washout was compared using the chi-square or Fisher's exact tests. The diagnostic ability to identify HCC, sensitivity, specificity, and accuracy of CEUS and Gd-EOB-MRI were calculated and compared using McNemar's test. Sample size was calculated with 80% power ( $\beta = 0.2$ ) and a significance level of 5% ( $\alpha = 0.05$ ) to reveal statistically significant differences in the diagnostic performance for HCC between CEUS and Gd-EOB-MRI (Supplementary Materials). Interobserver agreement of the imaging features between the operators and reviewer was

**Table 2. The Definition of Major Image Features and Diagnostic Criteria of EASL and KLCA-NCC Guidelines**

Modality	Guidelines	Image Features	Definition
Gd-EOB-MRI	EASL	APHE	Non-rim like enhancement in arterial phase unequivocally greater in whole or in part than liver
		Washout	Non-peripheral temporal reduction in enhancement in whole or in part relative to composite liver tissue, resulting in hypoenhancement on portal venous phase
		Diagnosis	≥ 1 cm observation with APHE and washout
	KCLCA-NCC	APHE	Enhancement in arterial phase unequivocally greater in whole or in part than liver
		Washout	Non-peripheral temporal reduction in enhancement in whole or in part relative to composite liver tissue, resulting in hypoenhancement on portal venous, delayed, or hepatobiliary phase
		Diagnosis	≥ 1 cm observation with APHE and washout. These criteria should be applied only to lesion which does not show either marked T2 hyperintensity or targetoid appearance on diffusion-weighted images or contrast-enhanced sequences
CEUS	EASL, KCLCA-NCC	APHE	Unequivocal enhancement compared to that of the liver parenchyma in the arterial phase and absence of rim-like or peripheral globular enhancement
		Washout	
		Definition	Visually assessed temporal reduction in enhancement in whole or in part relative to liver beginning in or after arterial phase and resulting in hypoenhancement
		Time	Early vs. Late washout: washout observed before or after 60 seconds
		Degree	Mild: the observation had less enhancement than the parenchyma, but not devoid of contrast, within 5 minutes after contrast injection
			Marked: the observation virtually becoming devoid of contrast within 2 minutes after contrast injection
		Diagnosis	≥ 1 cm observation with APHE followed by late (≥ 60 seconds) washout of mild degree (distinctive washout)

APHE = arterial-phase hyperenhancement, CEUS = contrast-enhanced ultrasound, EASL = European Association for the Study of the Liver, Gd-EOB-MRI = gadoxetate-enhanced MRI, KLCA-NCC = Korean Liver Cancer Association-National Cancer Center

analyzed by weighted  $\kappa$  statistics (Supplementary Materials). Statistical analyses were performed using MedCalc version 16.4 (MedCalc Software). Two-tailed  $p$  values < 0.05 were considered to indicate a statistically significant difference.

## RESULTS

### Participants and Hepatic Observations

The participants had liver cirrhosis (43.7%, 45/103), hepatitis B infection (65.0%, 67/103), or both (8.7%, 9/103) (Table 1). The clinicopathological characteristics of these observations are described in Table 1. The mean size of observations was  $28.2 \pm 24.5$  mm (range, 11–114 mm). More than three-quarters of lesions 76.7% (79/103) were confirmed as HCCs, with 14.6% (15/103) being non-HCC malignancies, and 8.7% (9/103) were benign lesions. The non-HCC malignancies were mostly intrahepatic CCs (73.3%, 11/15); however, there were two cases of combined HCC-CCs, a liver metastasis from the pancreatic neuroendocrine tumor, and an angiosarcoma. Benign lesions ( $n = 9$ ) included three dysplastic nodules, two adenomas, a hemangioma, a focal nodular hyperplasia, a regenerative

nodule, and an organizing hematoma.

Fifty-seven observation lesions (55.3%) were diagnosed histopathologically based on a surgical ( $n = 16$ ) or biopsy sample ( $n = 41$ ). In contrast, forty-six observation lesions (44.7%) were diagnosed based on characteristic imaging features of hemangioma ( $n = 1$ ) and HCC ( $n = 45$ ), according to the CT/MRI LI-RADS v2018 (1, 25).

### Major Imaging Features of Gd-EOB-MRI and CEUS

The major imaging features of the 103 observation lesions are summarized in Supplementary Table 2. There were two non-evaluable cases in CEUS even after real-time CT/MRI fusion due to a poor sonic window ( $n = 2$ ).

#### APHE

There was no significant difference in demonstrating APHE between Gd-EOB-MRI and CEUS (72.8% vs. 77.7%,  $p = 0.33$ ) (Supplementary Table 2). No HCC presented rim APHE on CEUS, while 5 HCCs showed rim APHE on Gd-EOB-MRI ( $p = 0.06$ ) (Table 3). Eight out of 10 (80%, 8/10) HCCs that did not show APHE on Gd-EOB-MRI further presented APHE when CEUS was used (Fig. 2). The interobserver

**Table 3. Comparison of APHE and Washout between Gd-EOB-MRI and CEUS**

Image Feature	Gd-EOB-MRI						
	All Hepatic Observations (n = 103)				HCCs (n = 79)		
	No APHE (n = 9)	APHE (n = 75)	Rim APHE (n = 18)	Peripheral Globular Enhancement (n = 1)	No APHE (n = 5)	APHE (n = 69)	Rim APHE (n = 5)
No APHE (n = 14)	6 (66.7)	6 (8)	3 (16.7)	0 (0)	2 (40)	6 (8.7)	0 (0)
APHE (n = 79)	3 (33.3)	69 (92)	8 (44.4)	0 (0)	3 (60)	63 (87.3)	5 (100)
Rim APHE (n = 7)	0 (0)	0 (0)	7 (38.9)	0 (0)	0 (0)	0 (0)	0 (0)
Peripheral globular enhancement (n = 1)	0 (0)	0 (0)	0 (0)	1 (100)	0 (0)	0 (0)	0 (0)
Concordance rate	83 (80.6)			65 (82.3)			

Numbers in parentheses are percentages.

agreement of APHE evaluation was excellent in Gd-EOB-MRI ( $\kappa = 0.85$ ) and good in CEUS ( $\kappa = 0.72$ ) (Table 3).

### Distinctive washout for HCC

Gd-EOB-MRI showed a more distinctive washout than CEUS (64.1% vs. 49.5%,  $p = 0.01$ ) (Supplementary Table 2). Among HCCs, 83.8% of Gd-EOB-MRI and 64.6% of CEUS cases presented distinctive washouts ( $p = 0.04$ ). None of the non-HCC observations presented a distinctive washout in CEUS. Apart from five HCCs with rim APHE on Gd-EOB-MRI, 12 HCCs did not present washout on PVP on Gd-EOB-MRI. Among these 12 HCCs, 8 (66.7%) showed distinctive washout on CEUS (Fig. 3). In addition, one HCC without an HBP defect on Gd-EOB-MRI presented a distinctive washout on CEUS. The interobserver agreement of distinctive washout was good in Gd-EOB-MRI ( $\kappa = 0.69$ ) and fair in CEUS ( $\kappa = 0.52$ ).

### Independent Comparison of the Diagnostic Ability for HCC between Gd-EOB-MRI and CEUS

The sensitivity, specificity, and accuracy of Gd-EOB-MRI and CEUS for diagnosing HCC among the at risk observations are summarized in Table 4 and Supplementary Table 3. The sensitivity of CEUS was lower than that of Gd-EOB-MRI with respect to the KLCA-NCC (60.8% vs. 86.1%,  $p < 0.01$ ) and EASL guidelines (60.8% vs. 72.2%,  $p = 0.06$ ). The specificities of Gd-EOB-MRI following the EASL guidelines were 95.8%, and the KLCA-NCC guidelines were 87.5%. CEUS yielded 100% specificity, which is significantly higher than that of Gd-EOB-MRI with the KLCA-NCC guidelines based on noninvasive diagnostic criteria ( $p = 0.04$ ).

Among the non-HCC lesions, there were no false-positive cases on CEUS. Compared to CEUS, there was one (by LI-RADS or EASL) and three (by KLCA-NCC) false-positive cases

on Gd-EOB-MRI, and these observations were re-categorized as non-HCC by CEUS (Fig. 4). The additional role of CEUS in false-positive and false-negative cases in Gd-EOB-MRI are shown in Table 5 and Supplementary Table 4.

### Subgroup Analysis

Among the fifty-seven pathologically confirmed observations, there were no statistical differences in the sensitivity between CEUS and Gd-EOB-MRI with respect to the KLCA-NCC guidelines (61.8% vs. 73.5%,  $p = 0.21$ ) or EASL guidelines (61.8% vs. 61.8%,  $p = 0.75$ ). The specificities of Gd-EOB-MRI following the EASL guidelines were 95.7%, and the KLCA-NCC guidelines were 86.9%. CEUS yielded 100% specificity.

### Diagnostic Ability of CEUS as a Second-Line Modality to Identify HCC among at Risk Observations

According to the EASL guidelines, 21 HCCs did not present imaging hallmarks (APHE and PVP washout) on Gd-EOB-MRI, of which 9 (42.9%) were further noninvasively diagnosed as HCC by using CEUS as a second-line diagnostic modality. Based on the KLCA-NCC guidelines, 11 HCCs did not present imaging hallmarks on Gd-EOB-MRI, among which 4 (36.4%) were further noninvasively diagnosed as HCC by using CEUS. Thus, sensitivity (EASL, 72.2% vs. 83.5%,  $p < 0.01$ ; KLCA-NCC, 86.1% vs. 91.1%,  $p = 0.04$ ) was significantly increased by adding CEUS for each guideline. The specificity was not changed by the addition of CEUS (Table 4). Representative cases are presented in Figures 3 and 4.

## DISCUSSION

In this study, we found that adding CEUS to Gd-EOB-MRI as a second-line diagnostic modality led to the diagnosis

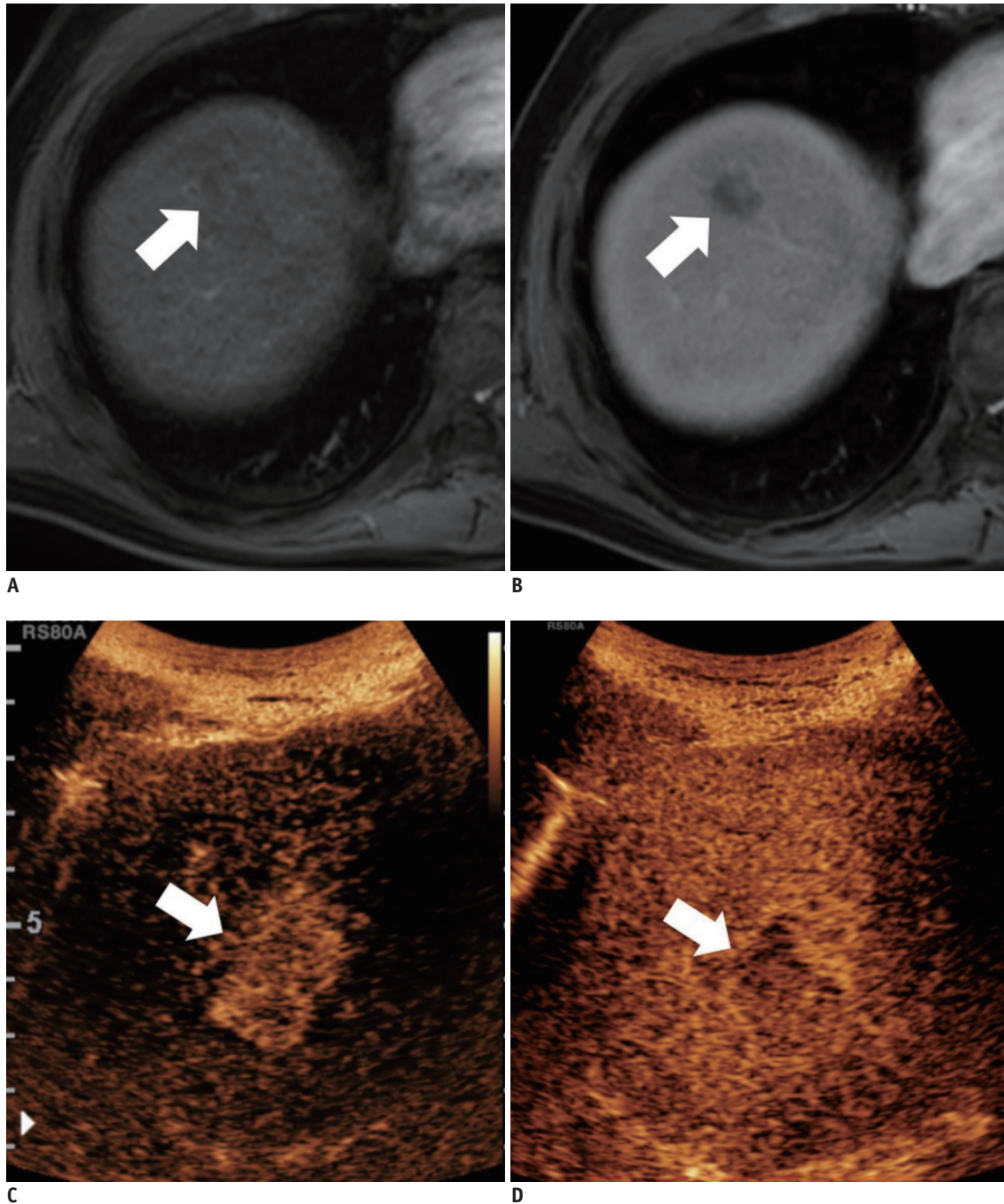


**Fig. 2. A 66-year-old man with chronic hepatitis B.**

(A) In the arterial phase of Gd-EOB-MRI, there was a 1.4-cm iso-enhancing observation (arrow) in segment 8 of the liver. This observation (arrow) presented washout on (B) the portal venous phase, which was inconclusive for a diagnosis of HCC. On CEUS, (C) a 1.6-cm APHE observation (arrow) was noted with mild washout at 87 seconds after contrast agent injection (D, arrow). This observation was concluded to reflect HCC, based on dynamic computed tomography images (APHE with portal washout) and elevated alpha fetoprotein level. APHE = arterial phase hyperenhancement

of more cases of HCC without lowering the specificity, according to the EASL and KLCA-NCC guidelines. In effect, we found that HCCs without APHE ( $n = 10$ ) or washout ( $n = 12$ ) on Gd-EOB-MRI further presented APHE (80%, 8/10) or washout (66.7%, 8/12) on CEUS, and no non-HCC lesions

further presented HCC imaging hallmarks in CEUS. This was not unexpected, given that the diagnostic algorithm of the EASL and KLCA-NCC guidelines indicated that CEUS could play a role after an initial, inconclusive MRI (5, 6). A previous study also reported that, after a first inconclusive

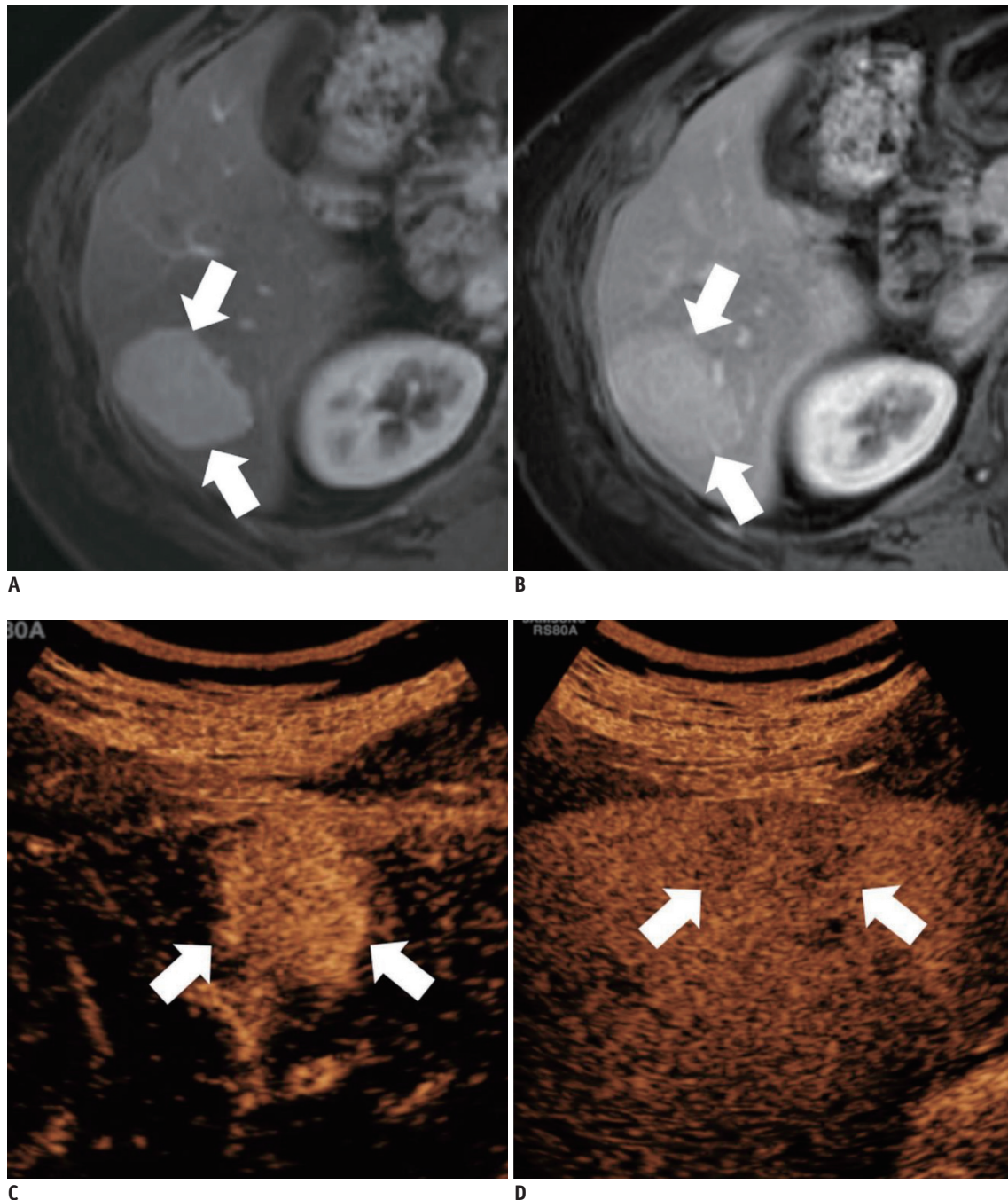


**Fig. 3. A 56-year-old man with pathologically confirmed HCC in segment 6 of the liver.** On Gd-EOB-MRI, (A) a 3.2-cm APHE observation (arrows) in segment 6 of the liver showed no washout in (B) the portal venous phase (arrows), which was thus inconclusive for diagnosing HCC. On CEUS, (C) a 3.2-cm APHE observation (arrows) was noted with a mild washout at 221 seconds after contrast agent injection (D, arrows).

MRI, CEUS, used as a second imaging technique, showed an increased sensitivity with only a slight reduction in specificity for 10–20 mm (7). Our study results supported the inclusion of CEUS as a second-line diagnostic modality, in addition to CECT and Gd-EOB-MRI, when the initial diagnostic test was inconclusive.

Various HCC imaging systems have been proposed, but there are still significant variations in their designs across geographic areas due to different target populations, resources, and treatment practices (4). However, it would be ideal for those organizations to use the same lexicon to describe imaging features obtained with the same

**Table 4. Diagnostic Ability of Gd-EOB-MRI with CEUS as a Second-Line Modality to Identify HCC among the at Risk Observations**

Guidelines	Gd-EOB-MRI			Gd-EOB-MRI, Then CEUS*			P		
	Sensitivity	Specificity	Accuracy	Sensitivity	Specificity	Accuracy	Sensitivity	Specificity	Accuracy
All (n = 103)									
EASL	72.2 (60.9, 81.7)	95.8 (78.9, 99.9)	0.84 (0.75, 0.90)	83.5 (73.5, 90.9)	95.8 (78.9, 99.9)	0.90 (0.82, 0.95)	< 0.01	N/A	< 0.01
KLCA-NCC	86.1 (76.5, 92.8)	87.5 (67.6, 97.3)	0.87 (0.79, 0.93)	91.1 (82.6, 96.4)	87.5 (67.6, 97.3)	0.89 (0.82, 0.95)	0.04	N/A	0.04
Noninvasive diagnostic criteria of CEUS <sup>†</sup>	CEUS with sulfur hexafluoride								
	60.8 (49.1, 71.6)	100 (85.8, 100)	0.80 (0.71, 0.88)						
Pathologic proven (n = 57)									
EASL	61.8 (43.6, 77.8)	95.7 (78.1, 99.9)	0.79 (0.66, 0.88)	76.5 (58.8, 89.3)	95.7 (78.1, 99.9)	0.86 (0.74, 0.94)	0.03	N/A	0.01
KLCA-NCC	73.5 (55.6, 87.1)	86.9 (66.4, 97.2)	0.80 (0.68, 0.90)	82.4 (65.5, 93.2)	86.9 (66.4, 97.2)	0.85 (0.73, 0.93)	0.08	N/A	0.04
Noninvasive diagnostic criteria of CEUS <sup>†</sup>	CEUS with sulfur hexafluoride								
	61.8 (44.6, 77.8)	100 (85.2, 100)	0.81 (0.68, 0.90)						

Numbers in parentheses are 95% confidence intervals. \*CEUS was performed when MRI presented inconclusive image features for noninvasive diagnosis of HCC. <sup>†</sup>Non-invasive diagnostic criteria of CEUS were APHE ( $\geq 1$  cm) with mild and late ( $\geq 60$  seconds) washout in CEUS LI-RADS v2017, EASL and KCLCA-NCC guideline.

diagnostic imaging modality (3). For example, for CECT and dynamic MRI, the HCC diagnostic criteria in the LI-RADS (1, 25), EASL (5), APASL (29), and KLCA-NCC (6) guidelines are quite universal, but they still disagree significantly in terms of the inclusion of CEUS in the HCC diagnostic algorithm.

In our study, CEUS detected less rim APHE than Gd-EOB-MRI, and no HCC presented rim APHE on CEUS. This may be due to the inherent superior sensitivity of US to microbubbles compared to the sensitivity of MRI to Gd contrast agent as well as the continuous real-time observation of CEUS during the arterial phase (11, 30, 31). However, mild and late ( $\geq 60$  seconds) washout of HCC was less frequently detected on CEUS than on Gd-EOB-MRI, perhaps causing the lower sensitivity of CEUS. In contrast, none of the benign or non-HCC malignancies presented mild and late ( $\geq 60$  seconds) washout in CEUS, resulting in high specificity. Moreover, one (by EASL) and three (by KLCA-NCC) false-positive cases in Gd-EOB-MRI were re-categorized as non-HCC observations by CEUS.

The CEUS HCC diagnostic criteria (APHE followed by late [ $\geq 60$  seconds], mild washout) used in our study provided 100% specificity. These criteria have now been adopted in CEUS LI-RADS v2017 (22), EASL v2018 (5), and KLCA-NCC v2018 (6). Our finding of 100% specificity by CEUS is in agreement with that of previous studies, in which refined criteria for HCC on CEUS provided extremely high

specificity and positive-predictive values for HCC diagnosis, and improved its capacity to differentiate malignant lesions, such as cholangiocarcinoma or metastases (5, 7, 22, 24). However, according to the EASL and KLCA-NCC guidelines, if the initial diagnostic test (CT or MRI) showed hallmark imaging features of HCC, the use of a second-line diagnostic modality is not recommended; hence, CEUS may not further increase specificity. Likewise, Khalili et al. (32) reported that single imaging scans have similar specificity to two coincidental positive scans, with much less resource utilization, for 1–2-cm nodules found on HCC surveillance. However, considering that one (by EASL) and three (by KLCA-NCC) false-positive cases in Gd-EOB-MRI were re-categorized as non-HCC observations by CEUS, the use of concurrent CEUS as a diagnostic test for HCC could be clinically valuable when high specificity is required, such as for liver transplantation (33). As these stringent criteria for HCC on CEUS are required to achieve such high specificity for HCC, but unavoidably lower sensitivity, further studies are necessary to find a way to combine an imaging modality with high sensitivity, with CEUS, with high specificity, in most clinical scenarios, except liver transplantation (34).

This study had several limitations. First, the small study sample size, especially the participants with benign lesions, was a limitation. This was partly because participants with benign nodules showing typical imaging features on CT

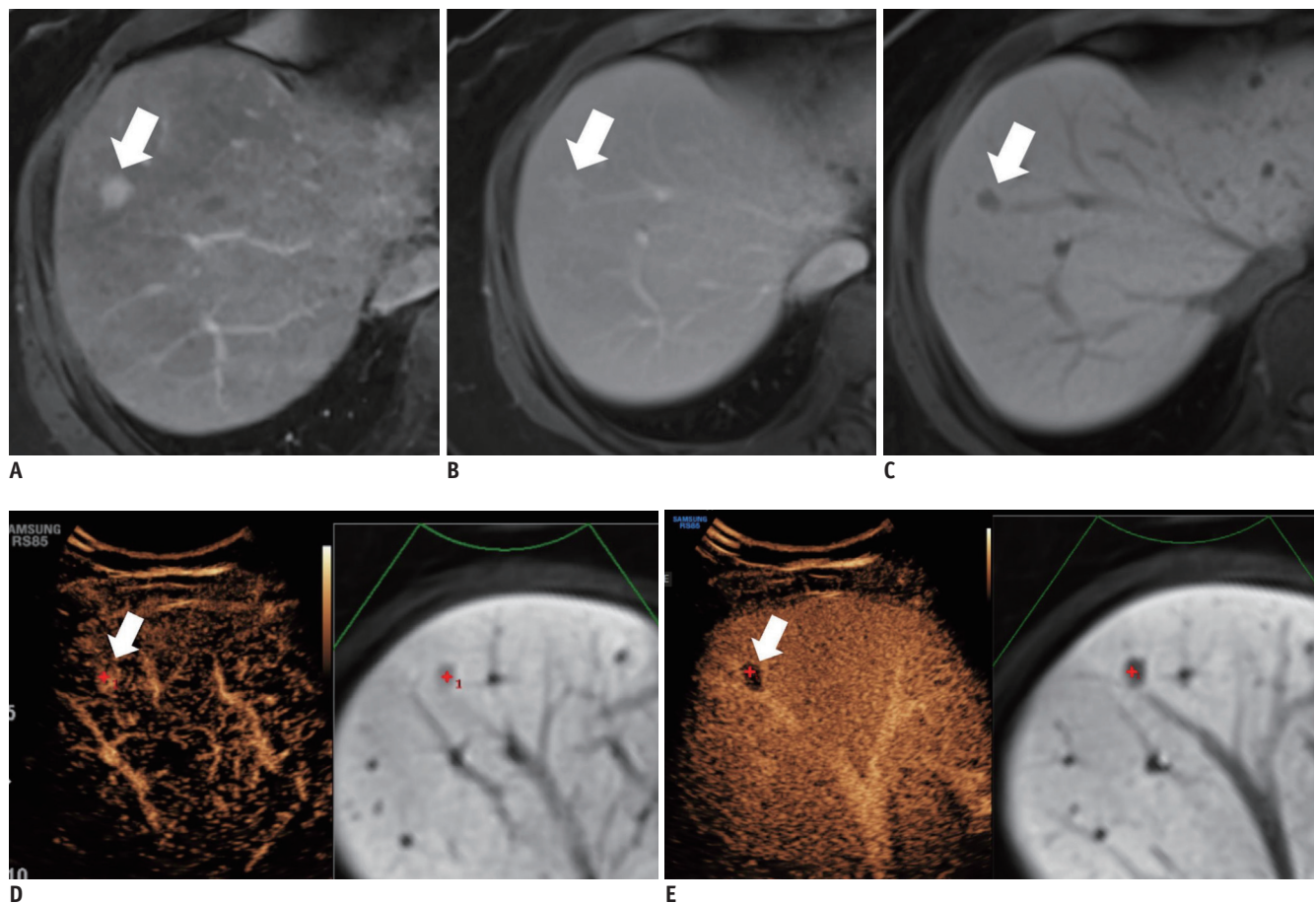


**Fig. 4. A 58-year-old woman with chronic hepatitis B and a pancreatic neuroendocrine tumor.** On Gd-EOB-MRI, (A) a 1.2-cm APHE observation (arrow) in segment 8 of the liver presented no washout (B) the portal venous phase (arrow) and hypointensity in (C) the hepatobiliary phase (arrow). Thus, this observation was noninvasively diagnosed as HCC using the Korean Liver Cancer Association and the National Cancer Center guidelines. On CEUS after real-time ultrasound image fusion with magnetic resonance image, (D) a 1.2-cm APHE observation (arrow) was noted early (48 seconds) and marked washout (E, arrow), which suggested malignancy other than HCC. This observation was confirmed as a hepatic metastasis from a pancreatic neuroendocrine tumor.

**Table 5. Additional Role of CEUS in False-Positive and False-Negative Cases in Gd-EOB-MRI**

	Gd-EOB-MRI	
	EASL	KLCA-NCC
HCCs (n = 79)	(-)	(-)
CEUS		
(-)	9 (11.4)	4 (5.1)
(+)	13 (16.5)	7 (8.9)
Non-HCCs (n = 24)	(+)	(+)
CEUS		
(-)	0 (0.0)	0 (0.0)
(+)	1 (4.2)	3 (12.5)

Numbers in parentheses are percentages. (+) refers to noninvasively diagnoses HCC.

or MRI seldom underwent CEUS in daily clinical practice. Second, there were several participants in whom imaging test results were used to establish a diagnosis without

histopathologic results. However, HCC is a unique neoplasm that can be diagnosed in high-risk patients using typical imaging features, and many patients with HCC are managed without pathologic confirmation. Liver mass biopsy tends to be performed on observation with atypical features. Therefore, to avoid selection bias, we also included noninvasively diagnosed HCC by dynamic CT. Third, many participants had chronic hepatitis B, which may limit the extent of extrapolation of our study results to participants with other etiologies accordingly.

In conclusion, the addition of CEUS to Gd-EOB-MRI as a second-line diagnostic modality significantly increased the sensitivity and diagnostic accuracy for diagnosing HCC among at risk observations, without changing specificities, following EASL v2018 and KLCA-NCC v2018 guidelines. Therefore, when the initial diagnostic test is inconclusive, our findings support the inclusion of CEUS as a second-line

diagnostic modality after CECT or dynamic MRI.

## Supplementary Materials

The Data Supplement is available with this article at <https://doi.org/10.3348/kjr.2020.0973>.

## Conflicts of Interest

The authors have no potential conflicts of interest to disclose.

## ORCID iDs

Hyo-Jin Kang

<https://orcid.org/0000-0002-6771-2112>

Jeong Min Lee

<https://orcid.org/0000-0003-0561-8777>

Jeong Hee Yoon

<https://orcid.org/0000-0002-9925-9973>

Joon Koo Han

<https://orcid.org/0000-0001-5916-5545>

## REFERENCES

- Marrero JA, Kulik LM, Sirlin CB, Zhu AX, Finn RS, Abecassis MM, et al. Diagnosis, staging, and management of hepatocellular carcinoma: 2018 Practice Guidance by the American Association for the Study of Liver Diseases. *Hepatology* 2018;68:723-750
- Cruite I, Tang A, Sirlin CB. Imaging-based diagnostic systems for hepatocellular carcinoma. *AJR Am J Roentgenol* 2013;201:41-55
- Tang A, Cruite I, Sirlin CB. Toward a standardized system for hepatocellular carcinoma diagnosis using computed tomography and MRI. *Expert Rev Gastroenterol Hepatol* 2013;7:269-279
- Tang A, Cruite I, Mitchell DG, Sirlin CB. Hepatocellular carcinoma imaging systems: why they exist, how they have evolved, and how they differ. *Abdom Radiol (NY)* 2018;43:3-12
- European Association for the Study of the Liver. EASL Clinical Practice Guidelines: management of hepatocellular carcinoma. *J Hepatol* 2018;69:182-236
- Korean Liver Cancer Association, National Cancer Center. 2018 Korean Liver Cancer Association-National Cancer Center Korea Practice Guidelines for the management of hepatocellular carcinoma. *Korean J Radiol* 2019;20:1042-1113
- Claudon M, Dietrich CF, Choi BI, Cosgrove DO, Kudo M, Nolsøe CP, et al. Guidelines and good clinical practice recommendations for contrast enhanced ultrasound (CEUS) in the liver--update 2012: a WFUMB-EFSUMB initiative in cooperation with representatives of AFSUMB, AIUM, ASUM, FLAUS and ICUS. *Ultraschall Med* 2013;34:11-29
- Aubé C, Oberti F, Lonjon J, Pageaux G, Seror O, N'kontchou G, et al. EASL and AASLD recommendations for the diagnosis of HCC to the test of daily practice. *Liver Int* 2017;37:1515-1525
- Strobel D, Bernatik T, Blank W, Schuler A, Greis C, Dietrich CF, et al. Diagnostic accuracy of CEUS in the differential diagnosis of small ( $\leq 20$  mm) and subcentimetric ( $\leq 10$  mm) focal liver lesions in comparison with histology. Results of the DEGUM multicenter trial. *Ultraschall Med* 2011;32:593-597
- Kim TK, Noh SY, Wilson SR, Kono Y, Piscaglia F, Jang HJ, et al. Contrast-enhanced ultrasound (CEUS) liver imaging reporting and data system (LI-RADS) 2017-a review of important differences compared to the CT/MRI system. *Clin Mol Hepatol* 2017;23:280-289
- Kang HJ, Kim JH, Joo I, Han JK. Additional value of contrast-enhanced ultrasound (CEUS) on arterial phase non-hyperenhancement observations ( $\geq 2$  cm) of CT/MRI for high-risk patients: focusing on the CT/MRI LI-RADS categories LR-3 and LR-4. *Abdom Radiol (NY)* 2020;45:55-63
- Itai Y, Furui S, Ohtomo K, Kokubo T, Yamauchi T, Minami M, et al. Dynamic CT features of arteriportal shunts in hepatocellular carcinoma. *AJR Am J Roentgenol* 1986;146:723-727
- Maruyama H, Takahashi M, Ishibashi H, Yoshikawa M, Yokosuka O. Contrast-enhanced ultrasound for characterisation of hepatic lesions appearing non-hypervascular on CT in chronic liver diseases. *Br J Radiol* 2012;85:351-357
- Yu JS, Kim KW, Jeong MG, Lee JT, Yoo HS. Nontumorous hepatic arterial-portal venous shunts: MR imaging findings. *Radiology* 2000;217:750-756
- Jang HJ, Kim TK, Wilson SR. Small nodules (1-2 cm) in liver cirrhosis: characterization with contrast-enhanced ultrasound. *Eur J Radiol* 2009;72:418-424
- Leoni S, Piscaglia F, Granito A, Borghi A, Galassi M, Marinelli S, et al. Characterization of primary and recurrent nodules in liver cirrhosis using contrast-enhanced ultrasound: which vascular criteria should be adopted? *Ultraschall Med* 2013;34:280-287
- Vilana R, Forner A, Bianchi L, García-Criado A, Rimola J, de Lope CR, et al. Intrahepatic peripheral cholangiocarcinoma in cirrhosis patients may display a vascular pattern similar to hepatocellular carcinoma on contrast-enhanced ultrasound. *Hepatology* 2010;51:2020-2029
- Li R, Zhang X, Ma KS, Li XW, Xia F, Zhong H, et al. Dynamic enhancing vascular pattern of intrahepatic peripheral cholangiocarcinoma on contrast-enhanced ultrasound: the influence of chronic hepatitis and cirrhosis. *Abdom Imaging* 2013;38:112-119
- Chen LD, Xu HX, Xie XY, Xie XH, Xu ZF, Liu GJ, et al. Intrahepatic cholangiocarcinoma and hepatocellular carcinoma: differential diagnosis with contrast-enhanced ultrasound. *Eur Radiol* 2010;20:743-753
- Wildner D, Bernatik T, Greis C, Seitz K, Neurath MF, Strobel

- D. CEUS in hepatocellular carcinoma and intrahepatic cholangiocellular carcinoma in 320 patients - early or late washout matters: a subanalysis of the DEGUM multicenter trial. *Ultraschall Med* 2015;36:132-139
21. Wildner D, Pfeifer L, Goertz RS, Bernatik T, Sturm J, Neurath MF, et al. Dynamic contrast-enhanced ultrasound (DCE-US) for the characterization of hepatocellular carcinoma and cholangiocellular carcinoma. *Ultraschall Med* 2014;35:522-527
  22. Kono Y, Lyshchik A, Cosgrove D, Dietrich CF, Jang HJ, Kim TK, et al. Contrast Enhanced Ultrasound (CEUS) Liver Imaging Reporting and Data System (LI-RADS®): the official version by the American College of Radiology (ACR). *Ultraschall Med* 2017;38:85-86
  23. Piscaglia F, Kudo M, Han KH, Sirlin C. Diagnosis of hepatocellular carcinoma with non-invasive imaging: a plea for worldwide adoption of standard and precise terminology for describing enhancement criteria. *Ultraschall Med* 2017;38:9-11
  24. Terzi E, Iavarone M, Pompili M, Veronese L, Cabibbo G, Fraquelli M, et al. Contrast ultrasound LI-RADS LR-5 identifies hepatocellular carcinoma in cirrhosis in a multicenter retrospective study of 1006 nodules. *J Hepatol* 2018;68:485-492
  25. Chernyak V, Fowler KJ, Kamaya A, Kielar AZ, Elsayes KM, Bashir MR, et al. Liver Imaging Reporting and Data System (LI-RADS) version 2018: imaging of hepatocellular carcinoma in at-risk patients. *Radiology* 2018;289:816-830
  26. Foucher J, Chanteloup E, Vergniol J, Castéra L, Le Bail B, Adhoute X, et al. Diagnosis of cirrhosis by transient elastography (FibroScan): a prospective study. *Gut* 2006;55:403-408
  27. Lim JK, Flamm SL, Singh S, Falck-Ytter YT; Clinical Guidelines Committee of the American Gastroenterological Association. American Gastroenterological Association Institute Guideline on the role of elastography in the evaluation of liver fibrosis. *Gastroenterology* 2017;152:1536-1543
  28. Kang HJ, Lee JM, Jeon SK, Ryu H, Yoo J, Lee JK, et al. Microvascular flow imaging of residual or recurrent hepatocellular carcinoma after transarterial chemoembolization: comparison with color/power Doppler imaging. *Korean J Radiol* 2019;20:1114-1123
  29. Omata M, Cheng AL, Kokudo N, Kudo M, Lee JM, Jia J, et al. Asia-Pacific clinical practice guidelines on the management of hepatocellular carcinoma: a 2017 update. *Hepatol Int* 2017;11:317-370
  30. Jang HJ, Kim TK, Burns PN, Wilson SR. CEUS: an essential component in a multimodality approach to small nodules in patients at high-risk for hepatocellular carcinoma. *Eur J Radiol* 2015;84:1623-1635
  31. Bolondi L, Gaiani S, Celli N, Golfieri R, Grigioni WF, Leoni S, et al. Characterization of small nodules in cirrhosis by assessment of vascularity: the problem of hypovascular hepatocellular carcinoma. *Hepatology* 2005;42:27-34
  32. Khalili K, Kim TK, Jang HJ, Haider MA, Khan L, Guindi M, et al. Optimization of imaging diagnosis of 1-2 cm hepatocellular carcinoma: an analysis of diagnostic performance and resource utilization. *J Hepatol* 2011;54:723-728
  33. Heimbach JK, Kulik LM, Finn RS, Sirlin CB, Abecassis MM, Roberts LR, et al. AASLD guidelines for the treatment of hepatocellular carcinoma. *Hepatology* 2018;67:358-380
  34. Kim TH, Yoon JH, Lee JM. Emerging role of hepatobiliary magnetic resonance contrast media and contrast-enhanced ultrasound for noninvasive diagnosis of hepatocellular carcinoma: emphasis on recent updates in major guidelines. *Korean J Radiol* 2019;20:863-879